Effects of Black Widow Spider Venom and Ca^{2+} on Quantal Secretion at the Frog Neuromuscular Junction

R. FESCE, J. R. SEGAL, B. CECCARELLI, and W. P. HURLBUT

From the Rockefeller University, New York, 10021; the Biophysics Laboratory, Veterans Administration Medical Center, New York 10010; and the Department of Medical Pharmacology and Center for the Study of Peripheral Neuropathies and Neuromuscular Diseases, University of Milan, CNR Center of Cytopharmacology, 20129 Milan, Italy

ABSTRACT A modification of the classical procedure of fluctuation analysis is used to measure the waveform, $w(t)$, mean amplitude, $\langle h \rangle$, and mean rate of occurrence, $\langle r \rangle$, of miniature endplate potentials (MEPPs) at frog cutaneous pectoris neuromuscular junctions treated with black widow spider venom (BWSV). MEPP parameters are determined from the power spectrum of the fluctuating potential and the second (variance), third (skew), and fourth semi-invariants (cumulants) of high-pass–filtered records of the potential. The method gives valid results even when the mean potential undergoes slow changes unrelated to MEPPs and when the MEPP rate is not stationary; it detects changes in the distribution of MEPP amplitudes and corrects for the nonlinear summation of MEPPs. The effects of Ca^{2+} on BWSV-induced secretion are studied in detail. When Ca^{2+} is absent, the power spectrum of the fluctuations is shaped like the spectrum of $w(t)$ and secretion is quasi-stationary; $\langle r \rangle$ rises smoothly to peak values of ~1,500/s and then quickly subsides to levels near 10/s. Many relatively small and some "giant" MEPPs occur at the ends of the experiments, and the distribution of MEPP amplitudes broadens. When the effects of this broadening are corrected for, we find that $\sim 0.7 \times 10^6$ MEPPs occurred during the 30 min of intense secretion. Since BWSV depletes nerve terminals of their quanta of transmitter and their synaptic vesicles, this figure is an upper limit for the quantal store in a resting terminal. When Ca^{2+} is present, the noise spectrum deviates from the spectrum of $w(t)$ and secretion is nonstationary; $\langle r \rangle$ rises to similar peak values but is sustained at levels near 400/s for up to an hour and at least 1.5×10^6 quanta are secreted within this period. Thus, the quantal store must have turned over at least twice under this condition. Data previously obtained at junctions treated with La^{3+} are corrected for nonlinear summation and for the distribution of MEPP amplitudes. The two corrections roughly compensate each other, and the corrected results confirm the previous conclusion that the number of quanta secreted from La^{3+}-treated terminals during 1 h is not strongly dependent upon the extracellular concentration of Ca^{2+}; $\sim 2 \times 10^6$ quanta are released even when Ca^{2+} is absent.

J. GEN. PHYSIOL. © The Rockefeller University Press · 0022-1295/86/07/0059/23 $1.00 59
Volume 88 July 1986 59–81

INTRODUCTION

Continuous measurements of the amplitude and rate of occurrence of miniature endplate potentials (MEPPs) during prolonged periods of vigorous secretion at neuromuscular junctions provide some of the basic data for testing the vesicle hypothesis of quantal secretion and for defining the kinetic properties of the processes that recycle synaptic vesicles and refill them with transmitter. Measurements made at junctions treated with black widow spider venom (BWSV) or its purified protein component, α-latrotoxin (α-LT), are especially interesting because these agents cause massive increases in the MEPP rate and deplete the nerve terminals of their synaptic vesicles and quantal store of acetylcholine (ACh) (Longenecker et al., 1970; Clark et al., 1972; Frontali et al., 1976; Gorio et al., 1978). The kinetics of secretion are strongly affected by the concentration of extracellular Ca^{2+} (Smith et al., 1977): the depletion of vesicles occurs quickly and most completely in Ca^{2+}-free solutions (Ceccarelli and Hurlbut, 1980). The rapid and complete depletion suggests that recycling is impaired, and therefore the measurement of the total number of MEPPs that occur in the absence of Ca^{2+} provides a useful estimate of the store of quanta in a resting terminal. Since the peak MEPP rates at these junctions are so great that the individual events cannot be resolved, they must be counted by other means. We use here a modification of classical fluctuation analysis (Segal et al., 1985; Fesce et al., 1986) to measure the MEPP rate as a function of time at frog neuromuscular junctions treated with BWSV or α-LT in Ca^{2+}-free or Ca^{2+}-containing solutions. The method is based upon Rice's (1944) generalization of Campbell's (1909) theorem to the higher semi-invariants of shot noise: $\lambda_n = \langle r \rangle h^n \int [w(t)]^n dt = \langle r \rangle h^n I_n$, where λ_n is the n^{th} semi-invariant of the noise, $\langle r \rangle$ is the mean shot rate, h is the shot amplitude, $w(t)$ is the shot waveform, and $I_n = \int [w(t)]^n dt$.

The shots at a vigorously secreting neuromuscular junction are the MEPPs. Their waveform is determined from the power spectrum of an unfiltered record of the fluctuating membrane potential, whereas their mean rate, $\langle r \rangle$, and the amplitude factor, $\langle h \rangle$, are computed from the second (variance), λ_2, and third (skew), λ_3, semi-invariants of a high-pass–filtered record of that potential. This modified procedure has four major advantages over the classical one, which uses λ_2 and the mean, λ_1: (*a*) it is unaffected by slow changes in membrane potential caused by factors other than the summation of MEPPs; (*b*) it yields valid results even when the MEPP rate is not stationary (Fesce et al., 1986); (*c*) it is less sensitive to the nonlinear summation of MEPPs, and the residual second-order errors that arise from this source can be readily corrected for, and (*d*) it corrects the estimates of $\langle r \rangle$ and $\langle h \rangle$ for the spread in the distribution of MEPP amplitudes, when secretion is stationary. The latter two corrections use measurements of the fourth semi-invariant, λ_4, of the fluctuations; they are of opposite sign and are approximately equal in magnitude when secretion is at its peak.

The results of these experiments are important for three reasons. First, they demonstrate unambiguously that more quanta are secreted from BWSV-treated terminals when the bathing solution contains Ca^{2+} than when it does not. This confirms a previous suggestion that the vesicles are recycled more extensively when Ca^{2+} is present (Ceccarelli and Hurlbut, 1980). Second, the measurement

of the total number of MEPPs recorded at BWSV-treated junctions in Ca^{2+}-free solutions sets a realistic upper limit for the number of quanta in a resting nerve terminal. This number has never been measured directly, in spite of its obvious importance for any meaningful analysis of the kinetics of quantal secretion. For instance, it should equal the number of synaptic vesicles in a terminal, if quanta are stored within these structures and released from them. Third, the results demonstrate that the modified procedure of fluctuation analysis can be applied under a wide variety of nonideal experimental conditions that preclude the use of the classical procedure. Some of these results have been published as an abstract (Fesce et al., 1985).

Previously published data obtained at La^{3+}-stimulated junctions are also corrected for nonlinear summation and the distribution of MEPP amplitudes (Appendix).

MATERIALS AND METHODS

Electrophysiology

Cutaneous pectoris muscles were dissected from frogs, *Rana pipiens*, and mounted in Lucite chambers that held either 0.7 or 2.7 ml of bathing solution. A neuromuscular junction was impaled with a glass micropipette filled with 3 M KCl (resistance, 10–30 MΩ), and the membrane potential was recorded with a conventional high-input impedance amplifier. A low-gain DC-coupled record (bandwidth, 0–1,250 Hz) and a high-gain AC-coupled record (bandwidth, 0.2–1,250 Hz) were stored on FM magnetic tape (model B, Vetter, Rebersburg, PA, or model 3964A, Hewlett-Packard Co., Palo Alto, CA) for later analysis by computer. Usually 3–10 min of baseline record was obtained before BWSV or α-LT was applied.

Simultaneous extra- and intracellular records were obtained from single junctions visualized through a microscope outfitted with interference-contrast optics. A micropipette filled with 2 M NaCl (resistance, 5–10 MΩ) was pressed against the surface of a junction to record extracellularly and a second micropipette was inserted into the underlying muscle fiber to record intracellularly. These signals were amplified (AC-coupled) and displayed on a dual-beam oscilloscope, and the traces were carefully examined to make sure that each extracellular MEPP coincided with an intracellular one. Both records were stored on magnetic tape (bandwidths, 3–2,500 Hz [extracellular record] and 0.2–2,500 Hz [intracellular record]). A low-gain DC-coupled record of the membrane potential was stored on the third channel of the tape recorder.

All the experiments were conducted at room temperature (20–24°C).

Solutions

The control solution contained (in mM): 116 Na^+, 2.1 K^+, 1.8 Ca^{2+}, 117 Cl^-, 2 HPO_4^{2-}, 1 $H_2PO_4^-$, pH 7.0. The muscles were always dissected and mounted in this solution, which was then replaced by one that contained, in addition, 4 mM Mg^{2+} and 10^{-7}–10^{-8} g/ml tetrodoxin (TTX). The Ca^{2+}-free solutions contained 1 mM EGTA and 4 mM Mg^{2+}. A few experiments were done with a solution that contained no Mg^{2+} and had been made hypertonic by the addition of sucrose (0.2 M, 6.8 g/100 ml).

Preparation of BWSV and Toxin

Heads of black widow spiders, *Latrodectus mactans tredecimguttatus*, were kept frozen at −40°C and small numbers (two to five) were thawed as needed. The glands were plucked

out and ground in a small volume of 0.12 M NaCl (1 gland/100 μl), and the homogenate was stored in the refrigerator for up to 2 wk. Small aliquots (10–100 μl) of the homogenate were added to the recording chamber (volume, ~2.7 ml), and the bath was gently stirred. The potency of a homogenate was checked in one experiment by measuring the reduction in the amplitude of the indirectly evoked compound action potential of the muscle: 100 μl of BWSV depressed the amplitude by 50% in 40 min and by 85% in 60 min. This blocking action of BWSV is equivalent to that produced by α-LT at a concentration of 1 μg/ml (Ceccarelli and Hurlbut, 1980), so that a gland contained ~2.7 μg of toxin. The dissociation constant, K_D, for the binding of α-LT to frog cutaneous pectoris muscle (at 0°C) is 2×10^{-9} M (Valtorta et al., 1984), and its molecular weight is $\sim 130 \times 10^3$ (Frontali et al., 1976). Thus, the effective concentrations of α-LT used in the experiments with crude BWSV ranged from 0.1 to 1 μg/ml, or 2–20 times the K_D.

α-LT, the purified active protein component of BWSV (Frontali et al., 1976), was a gift from Dr. Jacopo Meldolesi, Milan, Italy. It was stored at −40°C and used at a final concentration of ~1 μg/ml in 0.7-ml chambers.

Power Spectra

The data were analyzed with a digital computer (PDP 11/23 plus or 11/73, Digital Equipment Corp., Maynard, MA), and power spectra were calculated from the high-gain AC record at 2–10-min intervals throughout each experiment. Most spectra were a composite of two averaged spectra obtained by sampling overlapping sections of the tape at two different rates. These averaged spectra were computed from eight contiguous records, each of which contained 2,048 12-bit data points collected either at 500 Hz (slow: range, 0.25–250 Hz) or at 2,500 Hz (fast: range, 1.25–1,250 Hz). The signals were first passed through an eight-pole Butterworth low-pass active filter (Frequency Devices, Inc., Haverhill, MA) set at one-half the respective sampling frequency to reduce aliasing (Bendat and Piersol, 1971). The ends of each digitized record were cosine tapered to reduce the "leakage" of spectral components that arises from windowing, and a fast Fourier transform was performed. The eight resultant spectra were averaged, and the average baseline spectrum, which was computed from the recording obtained before the MEPP rate had risen noticeably, was subtracted.

When the spectral composition of a signal is unknown, it is usually recommended that the corner frequency of the anti-aliasing filter be set to 0.4–0.25 times the sampling rate (Bendat and Piersol, 1971; Eisenberg, 1983), rather than one-half this rate as we did. However, our experimental spectra were not much higher than baseline at frequencies above 500 Hz, which is less than one-fourth of our higher sampling rate, and they contained almost no power at frequencies above 250 Hz (Fig. 2). In a few cases, power spectra were computed from a given set of data, first with the filter set at one-half the sampling rate and then with it set at one-quarter the sampling rate. These spectra were indistinguishable and therefore aliasing did not influence our results. Setting the filter as close as possible to one-half the sampling rate makes maximum use of the data (Bendat and Piersol, 1971).

Determining the MEPP Time Constants

The MEPP waveform, $hw(t)$, is closely approximated by the difference between two exponentials (Segal et al., 1985):

$$hw(t) = h(e^{-t/\theta_1} - e^{-t/\theta_2}), \quad (1)$$

where θ_1 is the time constant of decay, θ_2 is the time constant of rise, and h is the amplitude factor. If MEPPs occur randomly at a constant mean rate, $\langle r \rangle$, then the power density,

$G(f)$, of the fluctuations has the shape of the product of two Lorentzians with corner frequencies $(2\pi\theta_1)^{-1}$ and $(2\pi\theta_2)^{-1}$ (Verveen and de Felice, 1974):

$$G(f) = G_0/[1 + (2\pi f\theta_1)^2][1 + (2\pi f\theta_2)^2], \quad (2)$$

where $G_0 = 2\langle r\rangle h^2(\theta_1 - \theta_2)^2$ is the low-frequency asymptote. When plotted on log-log coordinates, this theoretical spectrum is flat out to 10–20 Hz for the values of θ_1 and θ_2 characteristic of MEPPs, and it declines at high frequencies with a limiting slope of −4.

During the baseline period, $\langle r\rangle$ was ~1/s, and h, θ_1, and θ_2 were determined by fitting Eq. 1 to the waveform obtained by averaging 20–30 MEPPs (Segal et al., 1985). When $\langle r\rangle$ was high (>50/s), G_0, θ_1, and θ_2 were determined by fitting Eq. 2 to log-log plots of the power spectra. Since θ_1 and θ_2 differ by about an order of magnitude, the fitting could be done in two independent steps. When the rate was stationary, the low-frequency limb of the slow spectrum was flat, and G_0 and θ_1 were determined by fitting a Lorentzian to it out to ~200 Hz. This analytical curve was multiplied by a second Lorentzian, and θ_2 was determined by fitting the resulting double Lorentzian to the points of the fast spectrum above 200 Hz. The fitting was facilitated by displaying on a storage oscilloscope the power spectrum, the analytic function, and the difference between the two. The parameters were adjusted until the difference was symmetric about zero across the entire spectrum, as judged by eye. The spectral points beyond 500 Hz sometimes fell below the analytic curve, but this is not a serious defect since the power densities at these frequencies are small and their contributions to the variance and skew are negligible.

When the MEPP rate was not constant, the low-frequency parts of the experimental spectra were not flat, and the densities continued to increase even at the lowest frequencies measured (0.25 Hz); all these spectra were shaped like double Lorentzians at frequencies above ~25 Hz, however. In these cases, G_0 and θ_1 were chosen by fitting the slow spectrum over the frequency range from ~20 to 200 Hz and the deviations of the experimental curve from the theoretical one at lower frequencies were ignored. Then θ_2 was determined as described above. After G_0, θ_1, and θ_2 had been chosen, the fast and slow power spectra were smoothed by frequency averaging as described previously (Segal et al., 1985); then they were combined at 200 or 250 Hz and plotted together with the fitted double-Lorentzian curve.

Semi-invariants

The recorded signals were first passed through a Butterworth low-pass filter set to 1,250 Hz and then through a high-pass RC filter (filter time constant, 1–5 ms) before being led to the computer. The filtered signal was digitized at 2,500 Hz and the second (variance), third (skew), and fourth semi-invariants of 10-s samples of data (25,000 points) were computed (2–5 s computation time). This process was repeated every 12–15 s until the entire tape had been analyzed. The semi-invariants of three successive samples were averaged and their mean baseline values were subtracted. The latter were the averages of 10–30 values computed from data samples collected before the rate had begun to rise. The differences were used for further calculation only when they were at least equal to their respective baseline values. These net values of the semi-invariants were then corrected for nonlinear summation using the equations (Fesce et al., 1986):

$$\lambda_2' = \lambda_2'(m) + 2[\lambda_3'(m)/V_d]\rho_3/\rho_2, \quad (3)$$

$$\lambda_3' = \lambda_3'(m) + 6\{[\lambda_2'(m)]^2/V_d\}(\rho_2{}^2/\rho_3) + 3[\lambda_4'(m)/V_d]\rho_4/\rho_3, \quad (4)$$

$$\lambda_4' = \lambda_4'(m) + 24[\lambda_2'(m)\lambda_3'(m)/V_d]\rho_2\rho_3/\rho_4, \quad (5)$$

where λ_n' is the corrected semi-invariant of a filtered record; $\lambda_n'(m)$ is the measured semi-

invariant of a filtered record; V_d is the mean driving potential for endplate current; $\rho_n = I'_n/I_n$; $I'_n = \int[w'(t)]^n dt$; and $w'(t)$ is the waveform of the filtered MEPP. These corrections were significant only for λ'_3 and λ'_4.

The mean MEPP rate, $\langle r \rangle$, and amplitude factor, $\langle h \rangle$, were computed from the variance, λ'_2, skew, λ'_3, and integrals of the filtered MEPPs using the following equations (Segal et al., 1985; Fesce et al., 1986):

$$\langle r \rangle = (\lambda'_2/I'_2)^3(I'_3/\lambda'_3)^2, \tag{6}$$

$$\langle h \rangle = (\lambda'_3/I'_3)(I'_2/\lambda'_2). \tag{7}$$

The ratio R, which monitors the spread in the distribution of h, was calculated from the equation:

$$R = (\lambda'_3/I'_3)^2/(\lambda'_2/I'_2)(\lambda'_4/I'_4). \tag{8}$$

The values of I'_n were determined as follows: the computer generated artificial MEPPs of the form $e^{-t/\theta_1} - e^{-t/\theta_2}$ using the values of θ_1 and θ_2 determined from power spectra. The simulated MEPPs were passed through the network used for data acquisition and returned to the computer, which calculated the integrals of the square, cube, and fourth power of the filtered events. The values of the integrals at other times were calculated by linear interpolation. All experiments were analyzed at least twice using filters with different time constants, τ (usually 1 and 2 ms), and the results were accepted only if they were independent of τ.

The accuracy of the measurements of λ_4 is subject to limitations similar to those that affect λ_3 (Segal et al., 1985; Fesce et al., 1986); the variability in its individual estimates increases as $\langle r \rangle$ increases and negative values are often obtained when $\langle r \rangle$ is near its peak. The variability and the number of negative values both decrease as the time constant, τ, of the filter is reduced, but the variability in the estimates of λ_4 always exceeds those in λ_3. The values of λ_4 used here were obtained with $\tau = 1$ ms. We emphasize that λ_4 was used only to correct the estimates of $\langle r \rangle$ and $\langle h \rangle$ for the effects of nonlinear summation and the distribution of amplitudes, and its effects on the former correction are small (Fesce et al., 1986). Its effects on R, on the other hand, are important (R is inversely proportional to λ_4), and therefore the estimates of R computed from 10-s samples of data tended to be highly variable. However, since the MEPP amplitude distribution does not change appreciably from moment to moment, we could correct the estimates of $\langle r \rangle$ and $\langle h \rangle$ using values of R averaged over several minutes of data in any given experiment and over several experiments at any given time (Figs. 6 and 7). The mean value of R is also highly dependent upon the corrections for nonlinear summation with uncorrected data consistently yielding seemingly unreasonable values ($R > 1$) when secretion was at its peak.

Interval Histograms of Extracellularly Recorded MEPPs

The computer continuously sampled the extracellular record at 2,500 Hz, recognized all events above a selected threshold, and displayed them so that spurious events could be rejected. Records were analyzed only when MEPP rates were ~3–20/s in order to avoid both excessively long sampling times and the frequent coincidence of more than one MEPP. Between 200 and 2,000 MEPPs were acquired for each histogram, depending on the rate of occurrence, and the intervals between successive MEPPs were plotted together with the theoretical probability distribution, $p(t)$, for random Poisson occurrences as computed from the mean interval, T: $p(t) = (1/T)e^{-t/T}$.

MEPP Amplitude Histograms

Portions of experiments where the MEPP rate was low enough to resolve individual events were analyzed. Digitized unfiltered records were displayed, and the peak amplitudes of

~100 MEPPs were measured. The baseline for an isolated MEPP was determined either by linearly extrapolating the values that prevailed just before it occurred or by joining the values before and after. Events with notches or inflections on their rising phases were counted as multiple events. Amplitudes could not be measured reliably when the MEPP rate exceeded ~100/s. If individual MEPPS are described by Eq. 1, the peak amplitude is proportional to h and the two parameters are distributed identically.

Results are reported as mean values ± SD.

RESULTS

Effect of Ca^{2+} on BWSV-induced Secretion

Fig. 1, *A* and *B*, shows strip-chart records of the changes in membrane potential at two endplates after the addition of 25 μl of BWSV to the bathing solution. One endplate (*A*) was in a muscle bathed in a modified Ringer's solution with no Ca^{2+}, 1 mM EGTA, and 4 mM Mg^{2+}, and the other (*B*) was in a muscle bathed in a modified Ringer's solution with 4 mM Mg^{2+}.The broadening of the trace indicates an increase in the MEPP rate. When Ca^{2+} was absent, the membrane potential declined gradually, while the MEPP rate rose smoothly to a peak; then the MEPP rate declined to very low values over the next 20 min, while the membrane potential recovered toward its original level. When Ca^{2+} was present, the decrease in membrane potential and the increase in the MEPP rate followed more ragged time courses, and although the MEPP rate declined from its peak value, it remained high throughout the period illustrated and still exceeded 400/s at the end. The raggedness of the fluctuations in membrane potential was clearly associated with bursts of MEPPs (compare Fig. 1, *C* and *D*). Del Castillo and Pumplin (1975) previously reported that MEPPs occurred in bursts at frog junctions treated with brown widow spider venom. Such nonstationarities in the MEPP rate distort the power spectrum and contribute to the variance and skew, thereby precluding the direct calculation of h and $\langle r \rangle$ from these semi-invariants.

Fig. 2 shows power spectra obtained at various times during the course of secretion at the junctions illustrated in Fig. 1. The spectra from the junction in the Ca^{2+}-free solution correspond closely to the spectrum of an MEPP, which indicates that the MEPP rate is quasi-stationary and that BWSV does not alter the MEPP waveform, activate extraneous sources of noise, or induce correlations among MEPPs. The spectra from the junction treated with BWSV and Ca^{2+}, on the other hand, deviate markedly from the MEPP spectrum at frequencies below 20 Hz, especially during the early minutes of secretion. The highly nonstationary bursting pattern of secretion that prevails when Ca^{2+} is present will add extra frequency components to the power spectrum (Rice, 1944; Fesce et al., 1986), but since many other factors also can contribute extra components (Schick, 1974), it is important to obtain independent evidence for nonstationary MEPP rates at neuromuscular junctions treated with BWSV, especially when the MEPP rate is high and the bursting is not obvious. This was done by recording extracellularly from limited regions of the neuromuscular junction and determining the distribution of intervals between successive MEPPs.

Interval Histograms of Extracellularly Recorded MEPPs

Fig. 3, *A–D*, shows power spectra computed from intracellular records at junctions treated with α-LT (*A*, no Ca^{2+}; *B*, with Ca^{2+}), a hypertonic solution (*C*), or

La^{3+} with Ca^{2+} (*D*); panels *E–H* show the interval histograms of the MEPPs recorded extracellularly from the same junctions. The spectrum from the junction treated with α-LT in Ca^{2+}-free solution is not distorted, and the interval histogram declines along the exponential curve expected for a Poisson process. Both results indicate that the MEPP rate was stationary over the data-collection

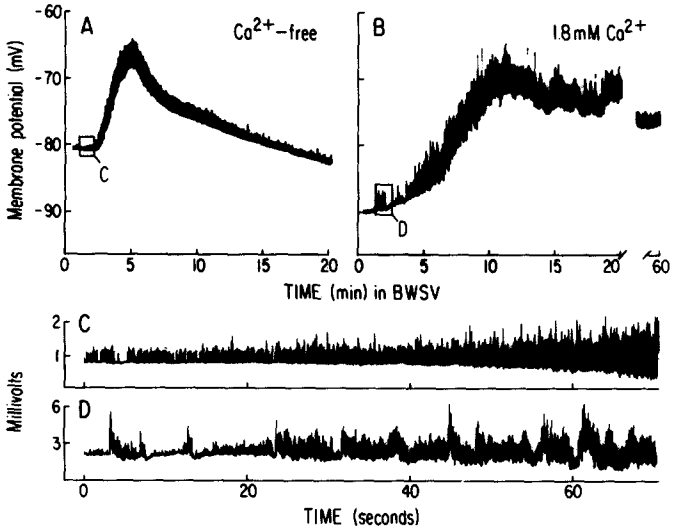

FIGURE 1. Strip-chart records of the changes in membrane potential at two neuromuscular junctions after the addition of 25 μl of BWSV. (*A* and *C*) Junction in Ca^{2+}-free Ringer's solution with 4 mM Mg^{2+} and 1 mM EGTA. (*B* and *D*) Junction in Ringer's solution plus 4 mM Mg^{2+}. Ordinates: millivolts; DC recording (*A* and *B*); AC recording ($\tau \sim 1$ s; *C* and *D*). Abscissae: time in minutes (*A* and *B*) or in seconds (*C* and *D*). BWSV was added at about −5 min, and 7–10 min later the membrane potential began to fall and $\langle r \rangle$ began to rise at both junctions. The rise in $\langle r \rangle$ is indicated by the broadening of the trace. The membrane potential of the junction in the Ca^{2+}-free solution had recovered to its original level by ~25 min and $\langle r \rangle$ had subsided to low levels, but at the other junction the membrane potential remained low and $\langle r \rangle$ remained high until 60 min. (Note break in time scale of *B*.) *C* and *D* show the early parts of the experiments (indicated by the boxes) displayed on a faster time scale and at higher gain (AC-coupled). In *C* (Ca^{2+} absent), $\langle r \rangle$ rose smoothly, but it fluctuated markedly in *D* (Ca^{2+} present).

interval. Similar results were obtained in six experiments in which α-LT or BWSV was applied in Ca^{2+}-free solution.

The spectrum obtained at the junction treated with BWSV and Ca^{2+} is distorted, and the MEPP intervals are not distributed exponentially. There was an excess of intervals shorter than 0.1 s, which is consistent with an intermittent, bursting pattern of quantal secretion. Similar results were obtained with all 3 histograms and spectra from this experiment and in 10 of the 12 histograms and spectra from all the junctions treated with α-LT or BWSV in solutions with Ca^{2+}.

Non-Poisson interval distributions were obtained whenever the power spectra were deformed.

The power spectrum obtained at the junction in hypertonic solution was distorted also, but the intervals between the extracellularly recorded MEPPs were distributed exponentially. This suggests that the spectral distortions seen

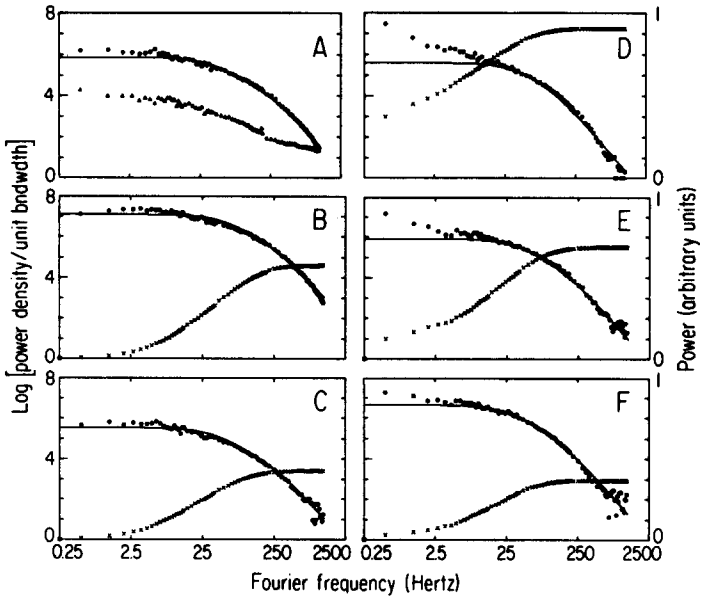

FIGURE 2. Power spectra obtained at the beginning (*A* and *D*), peak (*B* and *E*), and end (*C* and *F*) of the experiments illustrated in Fig. 1. (*A–C*) Ca^{2+}-free solution; (*D–F*) solution with 1.8 mM Ca^{2+}. Ordinate: power per unit bandwidth, arbitrary units, log scale; or total power, arbitrary units, linear scale. Abscissae: Fourier frequency (Hz), log scale. ●: power density during secretion, baseline subtracted; ▲: power density of baseline; ×: integral of power density; solid line: double Lorentzian. The three spectra in the Ca^{2+}-free solution are well fit by this curve, whereas the other spectra deviate markedly from it at frequencies below 25 Hz. The integrals show that these low-frequency components make large contributions to the variance, especially in the early stages of secretion. The time constants (milliseconds) of the fitted Lorentzians and the times (minutes) at which the spectra were computed are: (*A*) $\theta_1 = 4.94$, $\theta_2 = 0.46$, $t = 7$ min; (*B*) $\theta_1 = 3.53$; $\theta_2 = 0.46$, $t = 9.5$ min; (*C*) $\theta_1 = 4.94$, $\theta_2 = 0.55$, $t = 23$ min; (*D*) $\theta_1 = 7.86$, $\theta_2 = 1.27$, $t = 11.5$ min; (*E*) $\theta_2 = 5.16$, $\theta_2 = 0.91$, $t = 18.5$ min; (*F*) $\theta_1 = 6.93$, $\theta_2 = 1.08$, $t = 60.5$ min.

at this junction were not due to nonstationarities in the MEPP rate. The spectrum and the interval histogram obtained at the junction in La^{3+} with Ca^{2+} were both well behaved, which indicates that secretion was stationary in this solution (Segal et al., 1985).

It is clear that a nonstationary rate may not be the only cause of the spectral distortions seen with BWSV and Ca^{2+}. However, the consistency between the

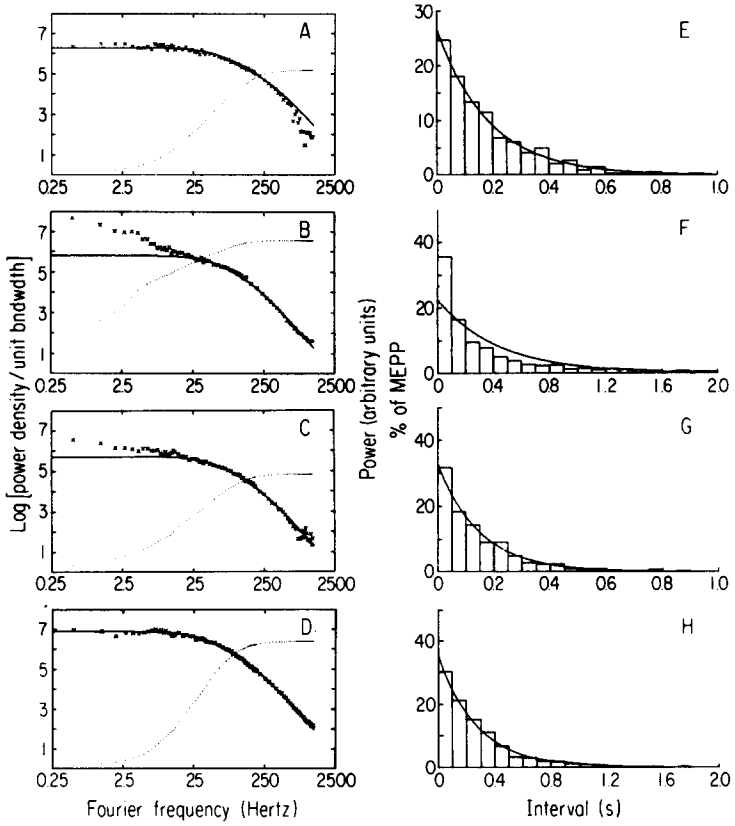

FIGURE 3. Intracellular power spectra and interval histograms of extracellularly recorded MEPPs. (*A–D*) Power spectra of intracellularly recorded fluctuations in potential at four different junctions. Ordinates: spectral density (arbitrary units), log scale, or power (arbitrary units), linear scale. Abscissae: Fourier frequency (Hertz), log scale. ×: spectral density; solid curve: double Lorentzien; dotted curve: integral of spectral density. (*A*) Junction treated with α-LT (1 μg/ml) in Ca^{2+}-free solution (10 min). (*B*) Junction treated with α-LT (1 μg/ml) in Ringer's solution with 4 mM Mg^{2+} (20 min). (*C*) Junction in hypertonic Ringer's solution with 200 mM sucrose (30 min). (*D*) Junction in Ringer's with 0.1 mM La^{3+} (4 min). The time constants (ms) of the fitted Lorentzians were: (*A*) 3.4 and 0.39; (*B*) 3.84 and 0.65; (*C*) 3.53 and 0.81; (*D*) 5.38 and 0.84. The variances, Var_m, determined from the integrals of the spectra and the expected stationary variances, Var_s, computed by integrating the Lorentzians were: (*A*) $Var_m = 39G_0$, $Var_s = 40.2G_0$; (*B*) $Var_m = 300G_0$, $Var_s = 57.6G_0$; (*C*) $Var_m = 55.7G_0$, $Var_s = 73.2G_0$; (*D*) $Var_m = 38.4G_0$, $Var_s = 40.2G_0$, where G_0 is the low-frequency asymptote of the fitted Lorentzian. Panels *E–H* show the interval histograms of MEPPs recorded extracellularly from these same junctions at the times the intracellular records for the power spectra were obtained. Ordinates: percent of intervals in each time bin. Abscissae: mean time of bin. The continuous line is an exponential computed from the mean interval, *T*: $p(t) = (1/T)e^{-t/T}$. The number of MEPPs and the mean intervals were: (*E*) 900 MEPPs, $T = 0.19$ s; (*F*) 2,000 MEPPs, $T = 0.22$ s; (*G*) 700 MEPPs, $T = 0.30$ s; (*H*) 800 MEPPs, $T = 0.28$ s. Note that the intervals are distributed exponentially in the hypertonic solution while the power spectrum is distorted.

spectra and the interval histograms obtained with this condition and the good behavior of both when Ca^{2+} was absent indicate that a major part of the distortion was due to bursting. Therefore, we used the filtering procedure described in the companion article (Fesce et al., 1986) to analyze the experimental records. Since filtering also removes low-frequency components arising from extraneous noise or correlations among MEPP parameters, our results will be valid even if these other complications are also present.

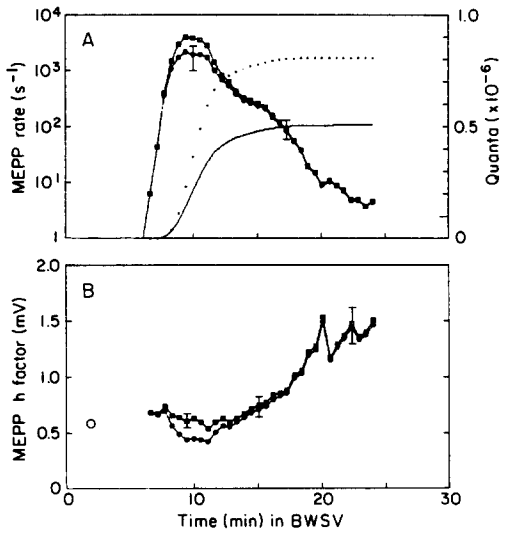

FIGURE 4. Effect of nonlinear summation on values of $\langle r \rangle$, h, and Q, the cumulative number of quanta secreted, at a single junction in the Ca^{2+}-free solution. Ordinates: (*A*) $\langle r \rangle$, log scale, or Q, linear scale; (*B*) h factor (millivolts). Abscissae: time (minutes) after adding BWSV. (*A*) Open symbols and dotted line: values before correction; solid symbols and line: values after correction. (*B*) Solid symbols: values before correction; open symbols: values after correction. The corrections are significant only when $\langle r \rangle$ exceeds ~400/s, but they reduce Q by ~50%. Estimates of $\langle r \rangle$ and h were made at a rate of ~4/min, and each point in this figure is the average of three of these. The error bars were computed by taking the standard deviations of the 8–10 individual estimates made over 2-min intervals and dividing by $3^{1/2}$. These errors (as percent of the means), for $\langle r \rangle$, were: 23% at the peak, 9.5% at 15 min, and 14% at 20 min; for h, they were 3.4% at the peak, 6.7% at 15 min, and 8.5% at 21 min. The first point in *B* (3 min, O) is the value of h determined by averaging the waveforms of 30 individual MEPPs collected while $\langle r \rangle$ was low.

Effect of Ca^{2+} on Quantal Secretion Induced by BWSV

Fig. 4 illustrates the changes in h, $\langle r \rangle$, and the number of quanta secreted, Q, at the junction illustrated in Fig. 1*A*. The open squares and the dotted line show the results obtained when $\langle r \rangle$, h, and Q are calculated directly from the variance and skew; the solid circles and line show the results obtained after correcting for nonlinear summation. The corrections are significant only when $\langle r \rangle$ exceeds 500/s; they reduce the peak values of $\langle r \rangle$ by ~42%, increase the corresponding values of h by 36%, and reduce Q by ~38%.

Fig. 5 and Table I summarize the results (corrected for nonlinear summation) of all our experiments with BWSV. Since similar results were obtained at doses ranging from 10 to 100 μl of BWSV/chamber, the data have been grouped only according to whether or not Ca^{2+} was present. In both solutions, $\langle r \rangle$ began to increase ~6 min after BWSV was applied, and 3–7 min later it reached peak values of ~1,600/s. The membrane potential declined by 13–18 mV as $\langle r \rangle$ approached its peak and then recovered partially; θ_1 decreased by 35–40% at the peak of secretion and also recovered partially; θ_2 did not change noticeably.

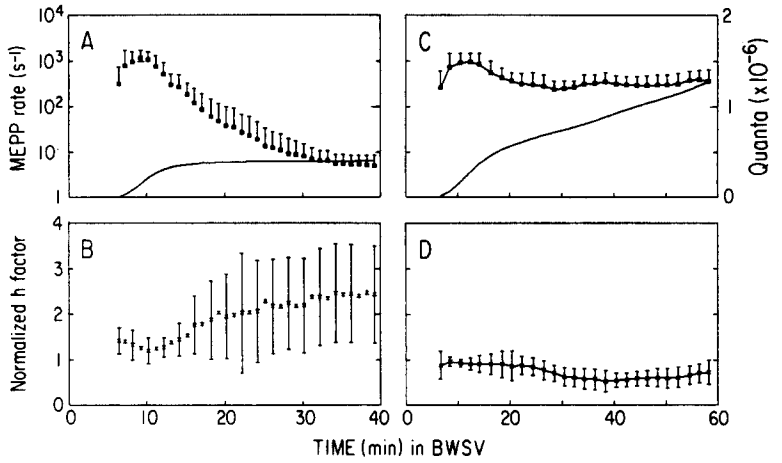

FIGURE 5. Average of the results of all experiments with BWSV. Data were corrected for nonlinear summation. (*A* and *B*) Experiments in the Ca^{2+}-free solution: eight junctions were followed for 12 min (i.e., through the peak), and seven of them for ≥17 min (i.e., until $\langle r \rangle$ had fallen to ≤10/s). (*C* and *D*) Experiments in the solution with Ca^{2+}; nine junctions were followed for 20–30 min (i.e., through the peak), and seven of these were followed for ≥60 min. Ordinates: (*A* and *C*) $\langle r \rangle$ (squares), log scale, or *Q* (continuous line), linear scale; (*B* and *D*) *h* factor (x's) normalized to the value determined from the average waveform of 20–30 individual MEPPs collected while $\langle r \rangle$ was low. Abscissae: time (minutes) after adding BWSV. Note differences between time scales. The large scatter of the results reflects differences among the junctions rather than measurement errors (compare with Fig. 4). The scatter was reduced by aligning the graphs to the time when $\langle r \rangle$ first exceeded 5/s. The apparent large increase in $\langle h \rangle$ in the Ca^{2+}-free solution is due primarily to the broadening of the MEPP amplitude distribution (see text).

The principal effects of Ca^{2+} were to sustain $\langle r \rangle$ at high levels and increase the number of quanta secreted. When Ca^{2+} was absent, $\langle r \rangle$ fell rapidly from its peak and $0.42 \pm 0.13 \times 10^6$ quanta were secreted by the seven junctions that were observed for 30 min or more. (One impalement was lost ~12 min after secretion had begun; by this time, $\langle r \rangle$ had fallen to below 10% of its peak value and 0.33×10^6 quanta had been secreted.) When Ca^{2+} was present, $\langle r \rangle$ was sustained at ~500/s at five of the seven junctions that were followed for 1 h; it had fallen below 50/s at the other two. A total of $1.36 \pm 0.50 \times 10^6$ quanta were secreted by these seven junctions over 1 h. This is significantly more secretion ($t = 4.2$, P

< 0.001) than in the Ca^{2+}-free solution. (About 1.5×10^6 quanta were secreted by the five junctions that were still active at 60 min; three of these were followed until 75 min, by which time they had secreted almost 2×10^6 quanta.) Similar results (not shown) were obtained when α-LT was applied at a concentration of 1 μg/ml, a dose roughly equivalent to the highest dose of BWSV.

TABLE I

Effect of BWSV on MEPP Parameters and Quantal Secretion

Parameter	Time	0 mM Ca^{2+}, 4 mM Mg^{2+}, 1 mM EGTA		1.8 mM Ca^{2+}, 4 mM Mg^{2+}	
Membrane potential	Control (mV)*	74±13	(8)	84±6	(9)
	Peak depolarization (mV)	13±4	(8)	18±6	(9)
	End depolarization (mV)	11±6	(7)	11±6	(7)
θ_1	Control (ms)*	5.9±1.8	(8)	7.2±2.0	(9)
	Start (%)	83±14	(8)	90±12	(9)
	Peak (%)	65±15	(8)	70±11	(9)
	End (%)	82±16	(7)	74±16	(7)
θ_2	Control (ms)*	0.61±0.28	(8)	0.66±0.33	(9)
	Start (%)	120±23	(8)	122±37	(9)
	Peak (%)	114±33	(8)	113±35	(9)
	End (%)	127±34	(7)	112±42	(7)
h	Control (mV)*	0.67±0.24	(8)	0.77±0.34	(9)
	Start (%)	136±24	(8)	88±22	(9)
	Peak (%)	123±28	(8)	81±14	(9)
	End (%)	236±102	(7)	63±23	(7)
$\langle r \rangle$	Peak (s^{-1})	1,500±700	(8)	1,600±580	(9)
	End (s^{-1})	5±4	(7)	360±225	(7)
$Q \times 10^{-6}$	End	0.42±0.13	(7)	1.26±0.50	(7)

Mean values ± SD. The number of junctions is given in parentheses. Results have been corrected for nonlinear summation.

* Control values were computed by curve-fitting the average of 20–30 MEPPs collected during the baseline period. Other values were determined by fluctuation analysis of data collected at the start, peak, or end of secretion. These values are given as a percent of the control values.

Changes in the Distribution of MEPP Amplitudes

The $\langle h \rangle$ factor changed little while $\langle r \rangle$ was rising toward its peak, but if Ca^{2+} was absent, it increased and ultimately reached values several times its initial value (Fig. 5). These late increases in $\langle h \rangle$ are due to "giant" MEPPs (Liley, 1957), which occurred relatively frequently at these late times (Kawai et al., 1972; Smith et al., 1977). They also occurred when Ca^{2+} was present, but then their effects were swamped by the far more numerous small MEPPs, and h remained low. Giant MEPPs broaden the distribution of MEPP amplitudes and cause $\langle h \rangle$ to be overestimated and $\langle r \rangle$ to be underestimated (Katz and Miledi, 1972; Finger and Stettmeier, 1981; Segal et al., 1985; Fesce et al., 1986). Since the size of these errors can be calculated from the moments of histograms of MEPP amplitude

(Fesce et al., 1986), we constructed these histograms for the five best (highest signal-to-noise ratio) experiments with the Ca^{2+}-free solution using data collected when $\langle r \rangle$ was low enough to observe individual MEPPs. The correction factor for $\langle r \rangle$ (i.e., the ratio of the "true" rate, $\langle r \rangle_t$, to the apparent rate, $\langle r \rangle$) varied from ~1.25 at the beginning of the experiments to >3 at the end. Since the

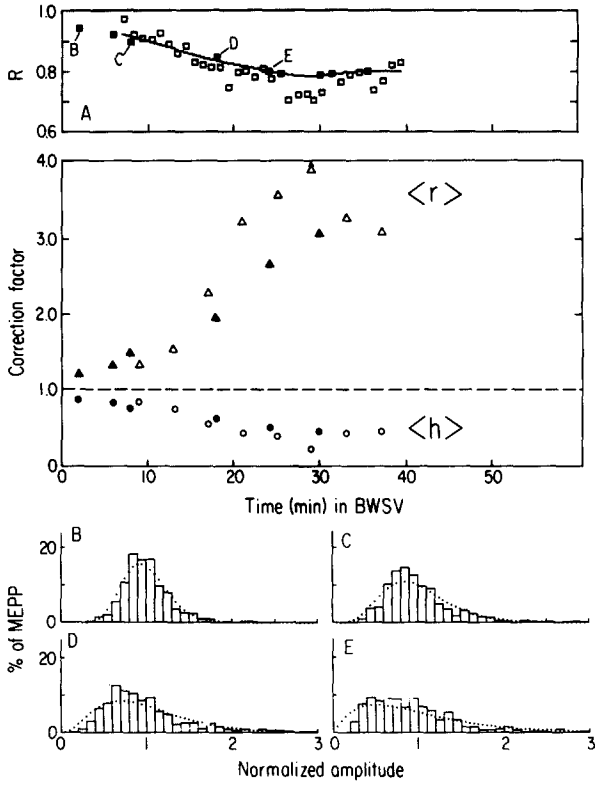

FIGURE 6. Changes in R, the correction factors for $\langle r \rangle$ and $\langle h \rangle$, and the MEPP amplitude histogram during BWSV-induced secretion in Ca^{2+}-free solution. Averaged results from five experiments. (*A*) Ordinates: R (squares) or correction factors for rate (triangles) and amplitude (circles); solid symbols are values computed from γ distributions fitted to the combined, normalized histograms; open symbols are values computed from the fluctuations. The latter values were computed from the averages of groups of four values of R. Abscissae: time (minutes) after adding BWSV. (*B–E*) Combined histograms obtained at various times in each experiment. Ordinates: fraction of MEPPs in each amplitude bin; abscissae: amplitude normalized to the mean amplitude. The dotted lines show γ distributions computed from the mean and variance of the histograms. The γ parameters and number of MEPPs in these histograms were: (*B*) γ = 13.3, 417 MEPPs (control); t = 6 min (not shown), γ = 8.7, 521 MEPPs; (*C*) γ = 5.5, 508 MEPPs; (*D*) γ = 2.4, 905 MEPPs; (*E*) γ = 1.03, 517 MEPPs; and t = 30 min (not shown), γ = 0.65, 380 MEPPs. The average values (millivolts) of the peak amplitudes of the control, early (<7 min), and late (>17 min) BWSV were, respectively, 0.48 ± 0.14, 0.45 ± 0.13, and 0.45 ± 0.10.

number of quanta secreted while $\langle r \rangle$ is near its peak constitutes a large fraction of the total number released, the error in this total can be estimated only if the amplitude distribution at these times is known. However, amplitude histograms cannot be constructed from data collected at the peak of activity because $\langle r \rangle$ is too great for individual MEPPs to be resolved, and one needs an index of the spread of the distribution of MEPP amplitudes (or h factors) that can be evaluated directly from the fluctuations. A suitable index is the ratio $R = [\lambda_3/I_3]^2/[\lambda_4/I_4][\lambda_2/I_2]$. R is independent or $\langle r \rangle$ and $\langle h \rangle$, and it estimates the ratio of the corresponding moments of the distribution of h: $\langle h^3 \rangle^2/\langle h^4 \rangle \langle h^2 \rangle$ (Fesce et al., 1986).

Fig. 6*A* shows how R changed with time during the five experiments from which the amplitude histograms were obtained. The combined, normalized MEPP amplitude histograms obtained at various times (*B–E*) are also shown. The values of R computed from the semi-invariants of the fluctuations (open squares) and those computed from the moments of the histograms (solid squares) are in excellent agreement, which is good evidence that R monitors the distribution of h. The gradual change in R with time shows that the distribution of h does not change drastically when $\langle r \rangle$ is at its peak.

TABLE II

Mean Values of $\langle h \rangle$, $\langle r \rangle$, and Q Corrected for the Distribution of MEPP Amplitudes

Parameter	Time	0 Ca^{2+}	1.8 mM Ca^{2+}*
h	Start	119	77
(% control)	Peak	92	71
	End	105	54
$\langle r \rangle$	Peak	2,300	1,940
(s^{-1})	End	17	440
Q	End	0.7×10^6	1.7×10^6

* These values were obtained using the initial values of the correction factors shown in Fig. 6.

The errors in $\langle r \rangle$ and $\langle h \rangle$ that arise from the distribution of MEPP amplitudes can be calculated from the moments of that distribution, or they can be calculated from R if the experimental distribution can be aproximated by an analytic function (Fesce et al., 1986). The histograms in Fig. 6 are fitted with γ functions: $p_\gamma(h) = \beta^{(\gamma+1)}h^\gamma e^{-\beta h}/\gamma!$ The γ parameter, as determined from the mean and variance of the histograms, changed from a value of 13 for the first (control) histogram to a value of 0.65 for the last (30 min) as the amplitude distribution changed from a near-Gaussian one with a coefficient of variation of 26% to a highly skewed one with a coefficient of variation near 80%. If it is assumed that γ functions fit the amplitude distributions throughout the course of secretion, then the correction factors for $\langle r \rangle$ and $\langle h \rangle$ can be calculated from the values of R (Fesce et al., 1986). The average values of these correction factors are also plotted in Fig. 6*A*; the rate-weighted average of the correction for $\langle r \rangle$ is 1.5.

Table II shows the results obtained when the mean values in Table I are

multiplied by these correction factors: the peak rate in the Ca^{2+}-free solution increased to ~2,000/s, and the total number of quanta secreted increased to $\sim 0.7 \times 10^6$. The apparent 2.5-fold increase in $\langle h \rangle$ seen in Fig. 5 and Table I is due almost entirely to the broadening of the amplitude distribution. This result agrees well with the results obtained directly from the amplitude histograms in that the mean amplitude remained almost constant, whereas the distribution broadened and its mode shifted to the left.

The values of R calculated from the experiments with Ca^{2+} showed great scatter, and their mean followed a complex time course. R was ~0.7 at the beginning of secretion, rose to 0.9 at the peak, fell to a minimum of 0.65 at 30 min, and rose again to ~0.9 at 60 min. These generally low values of R, especially those at the beginning of secretion, suggest that the nonstationarities in rate may have contaminated λ_4 (Fesce et al., 1986). Since no important changes in either the mean h or in the scatter of its values occurred in these experiments, it is likely that giant MEPPS never became frequent enough to seriously affect the amplitude distribution. If the initial values of the correction factors in Fig. 6 are applied to the data in Table I, then the values illustrated in Table II are obtained: the cumulative secretion during 1 h in BWSV with Ca^{2+} is 1.7×10^6 quanta.

DISCUSSION

Ca^{2+} has profound effects on the action of low doses of BWSV at the frog neuromuscular junctions (Smith et al., 1977; Ceccarelli and Hurlbut, 1980). When Ca^{2+} is absent, the MEPP rate quickly subsides from its peak values, and after an hour the terminals are swollen and depleted of their synaptic vesicles and releasable stores of transmitter (Longenecker et al., 1970; Clark et al., 1972; Gorio et al., 1978). When Ca^{2+} is present at its normal concentration, the MEPP rate remains high, transmission persists at many junctions, and the terminals retain most of their vesicles because they are recycled (Ceccarelli and Hurlbut, 1980). Since the peak MEPP rates could not be measured in these earlier experiments, it was not known whether the terminals in Ca^{2+} secreted more quanta or simply secreted them more slowly. The present results demonstrate unambiguously that, first, the peak rates of secretion are similar under the two conditions and, second, at least twice as many quanta are secreted when Ca^{2+} is present as when it is absent. These results are consistent with the view that the vesicles are recycled more effectively at BWSV-treated terminals when Ca^{2+} is present. The results with La^{3+} (Appendix) (Segal et al., 1985), showing that $\sim 2 \times 10^6$ quanta can be secreted in Ca^{2+}-deficient solutions, rule out the alternative interpretation that such solutions are deleterious to the terminals, causing vesicle loss or degradation of stored quanta even in the absence of secretion. However, the La^{3+} data do indicate that the apparently Ca^{2+}-dependent retention of vesicles seen with BWSV is related to the mechanism of action of the venom and is not a sign that Ca^{2+} plays a direct role in recycling. A similar conclusion was reached by Haimann et al. (1985), who found that vesicle recycling was impaired at ouabain-treated terminals even when Ca^{2+} was present. Recycling may fail at terminals treated with ouabain or BWSV because their ionic contents change: in

ouabain because the Na^+ pump is inhibited, and in BWSV because ionic permeability is increased (Finkelstein et al., 1976; Misler and Hurlbut, 1979; Nicholls et al., 1982; Meldolesi et al., 1984). The extracellular concentration of Ca^{2+} could influence recycling indirectly by affecting the size of the increase in permeability. Liscum et al. (1982) have observed that membrane circulation in frog photoreceptors is altered by agents that affect ionic permeability, and Larkin et al. (1983) found that depletion of intracellular K^+ inhibits receptor-mediated endocytosis in human fibroblasts.

Another important result of these experiments is the measurement of the total number of quanta secreted from terminals treated with BWSV in Ca^{2+}-free solutions. This number sets an upper limit for the store of quanta in a terminal at rest. Our value for it, 0.7×10^6, agrees well with the estimate of the number of synaptic vesicles in control terminals (Segal et al., 1985; Haimann et al., 1985) and also with the total number of quanta secreted from ouabain-treated terminals, where recycling is also inhibited (Haimann et al., 1985). However, this value will have to be revised downward if conditions are found under which the secretion of fewer quanta leads to exhaustion of the quantal stores. The giant MEPPs that are commonly seen after prolonged secretion induced by a variety of means may be a sign that the recycling process has failed and the terminal is near exhaustion. They may occur less frequently at BWSV-treated terminals when Ca^{2+} is present, or at La^{3+}-treated terminals, simply because recycling persists longer under these conditions.

Del Castillo and Pumplin (1975) suggested that the bursting pattern of secretion they observed at junctions treated with Ca^{2+} and brown widow spider venom was due to the local depletion of quanta from limited regions of the terminals. The bursting could also be due to the transient influx of Ca^{2+} through venom-induced channels in the nerve terminal axolemma. The duration of the bursts, on the order of a few seconds as judged from extracellular recordings, may be related to the kinetics of these channels, to the association and dissociation of individual toxin molecules with their receptor, or to the rate at which Ca^{2+} is cleared from the axoplasm.

Martin and Finger (1985) observed peak rates of excitatory miniature endplate currents (MEPCs) of $10–25 \times 10^3$/s and the release of $0.2–0.8 \times 10^6$ quanta during 120–170 s of secretion at voltage-clamped crayfish claw muscle fibers treated with 100 mM K^+. These figures represent the summed activity of ~1,900 release sites distributed over the surface of a fiber (Florey and Cahill, 1982; Finger, 1984), so the peak rate and total secretion per site are 5–12/s and 100–400 quanta, respectively. The latter figure is a few times larger than the number of synaptic vesicles in excitatory synapses in crayfish abdominal muscle (Nakajima and Reese, 1983). The 600-μm-long nerve terminals of frog cutaneous pectoris muscle (Letinsky et al., 1976; Valtorta et al., 1984) are comprised of ~600 active zones spaced ~1 μm apart (Peper et al., 1974). Thus, the peak rate and total secretion per active zone in our experiments in the Ca^{2+}-free solution were ~4/s and 1,200 quanta, respectively. A single active zone in frog terminals can secrete almost as rapidly as a single excitatory synapse in crayfish muscle, but stores several times as many quanta.

Changes in MEPP Amplitudes

The distribution of MEPP amplitudes broadened considerably during the experiments with BWSV and with La^{3+}, and the modes of the distributions declined by ~50% from the values during the early minutes of secretion (Figs. 6 and 7). Kriebel and Gross (1974) and Kriebel and Florey (1983) previously observed reductions in MEPP amplitude at frog neuromuscular junctions after electrical stimulation, exposure to elevated temperature, or treatment with La^{3+}. Carlson and Kriebel (1985) have suggested that a quantum is composed of ~10 subunits that account both for the multiple peaks they observed in the MEPP amplitude histograms and for the decline in MEPP amplitude that accompanies intense secretion. We cannot rule out such a possibility since our histograms contained too few MEPPs to reveal such peaks and the MEPP amplitudes were too small (~0.4 mV) to permit a small subclass of MEPPs (amplitude, ~0.04 mV) to be defined. We also cannot rule out the possibility that some of the reduction in amplitude was due to postsynaptic factors, but the broadening of the distribution should not be affected by such factors. However, as an alternative interpretation, we suggest that the broadening of the distribution and the decrease in its mode are due to vesicle recycling, which creates a heterogeneous population of vesicles filled to different degrees with transmitter (Katz, 1978). If small MEPPS are a sign of recycling, then it would appear that some recycling occurred in our experiments with BWSV in Ca^{2+}-free solution, so that the number of quanta released under this condition overestimates the initial store. On the other hand, it is possible that empty, or nearly empty, vesicles can recycle so that the turnover of vesicles exceeds the turnover of quanta (Ceccarelli and Hurlbut, 1975).

APPENDIX

La^{3+} Data

The recorded data from all 13 of our previously reported experiments with La^{3+} (Segal et al., 1985) were reanalyzed using a filter of 1 ms, and the semi-invariants were corrected for nonlinear summation; amplitude histograms and R factors were computed for the nine experiments with the best signal-to-noise ratios. The filter time constant is only ~60% of the average value of the time constant of rise of MEPPs in La^{3+} (1.6 ms), and in the late stages of several experiments, when r was low and h was small, the heavy filtering reduced the values of λ_2 to levels near the baseline, so that significant results could not be obtained. Reducing the filter time constant from 3 (the previous value used) to 1 ms did not significantly change the average peak rates, the average number of quanta secreted in 1 h, or the average initial values of the h factors. The La^{3+} solutions were buffered with Tris and contained no EGTA.

Table III presents the corrected results. Chauvinet's criterion (Mellor, 1955) was used to reject one experiment in the Ca^{2+}-deficient solution at 23°C because the final rates were six times the average of the final rates of the four others. The corrections for nonlinear summation reduced the peak rates by 58–67%, reduced the quantal outputs by 40–48%, and increased by 80–90% the values of h at the peak of secretion (not shown). The corrected peak rates were marginally lower when Ca^{2+} was present, but the final rates were significantly higher, in keeping with the significantly higher number of vesicles remaining in these preparations (Segal et al., 1985). The quantal outputs at 23°C were

similar with and without Ca^{2+}; both were comparable to the output in BWSV with Ca^{2+}, and both were several times larger than the output in BWSV without Ca^{2+} (Table I).

Fig. 7 presents the combined histograms of the distribution of MEPP peak amplitudes determined at various times during the nine experiments with the best signal-to-noise ratios. Histograms *C*, *D*, and *E* include data mostly from preparations in the Ca^{2+}-deficient solution, since $\langle r \rangle$ was too high in the others for the amplitudes to be measured. The histograms are well fitted by γ distributions and, although the distributions broaden (Kriebel and Florey, 1983), their spreads are smaller than those in BWSV because fewer

TABLE III

Corrected La^{3+} Data

	Corrected for nonlinear summation			Corrected for nonlinear summation and the distribution of MEPP amplitudes		
	Peak rate	End rate	$Q \times 10^{-6}$	Peak rate	End rate	$Q \times 10^{-6}$
	s^{-1}	s^{-1}		s^{-1}	s^{-1}	
0.1 mM La^{3+} 1.8 mM Ca^{2+} 4 mM Mg^{2+} 23°C ($N = 6$)	930±490*	244±118‡	1.5±0.56	1,900	300	3.5
0.1 mM La^{3+} 0 mM Ca^{2+} 4 mM Mg^{2+} 23°C ($N = 4$)	1,700±700*	30±18‡	1.1±0.28	3,800	60	2.7
0.2 mM La^{3+} 0 mM Ca^{2+} 4 mM Mg^{2+} 17°C ($N = 2$)	800±150	15±10	0.56±0.09	1,400	30	1.3

Mean values ± SD. N = number of junctions.

* Marginally significant difference ($t = 2.06$, $P \sim 0.08$).

‡ Significant difference ($t = 3.53$, $P < 0.01$).

giant MEPPs occur in La^{3+}. Fig. 7 also presents for these experiments the values of R determined from the fluctuations and those determined from the moments of the histograms. There is good agreement between the R factors computed from the histograms and those computed from the fluctuations recorded at junctions in the Ca^{2+}-deficient solution. The R factor was well-behaved in the solutions with Ca^{2+}, presumably because $r(t)$ was quasi-stationary (Fig. 3; Segal et al., 1985).

The right-hand side of Table III presents the results obtained when the mean values on the left were corrected for the distribution of amplitudes using these values of R and assuming that the amplitudes were distributed in accordance with γ functions. These final values are close to the previously reported uncorrected values (Segal et al., 1985). The final conclusion is that the terminals at 23°C secreted at peak rates near 2,000/s and

released >2 × 10^6 quanta during 1 h, even when Ca^{2+} was absent. These corrected data fully corroborate our direct demonstration with horseradish peroxidase that vesicle recycling occurs at La^{3+}-stimulated junctions in Ca^{2+}-free solutions (Segal et al., 1985).

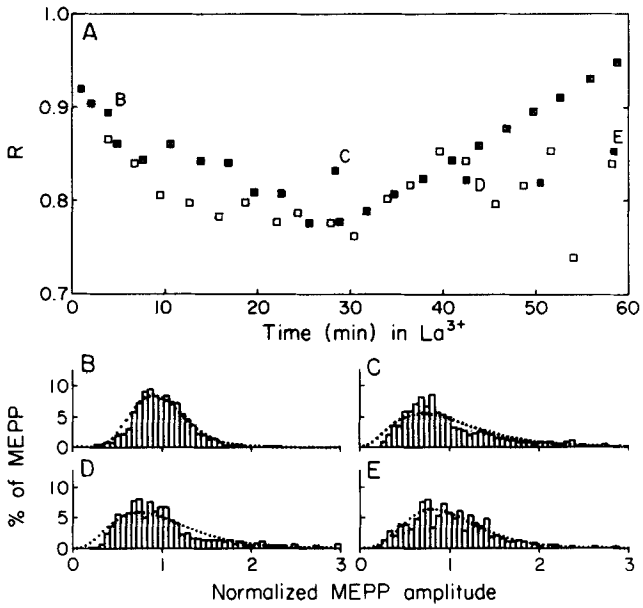

FIGURE 7. Changes in R and the MEPP amplitude histograms at junctions treated with 0.1 mM La^{3+}. Averaged results from nine experiments, five with Ca^{2+} and four without. Ordinates and abscissae as in Fig. 6. R computed from: □, fluctuations in 0 mM Ca^{2+}; ⊠, fluctuations in 1.8 mM Ca^{2+}; ■, moments of combined histograms. The times the data were collected and the γ parameters and number of MEPPs of the histograms were: control, t = 1 min (not shown), γ = 10.4, 1,237 MEPPs; (*B*) t = 4 min, γ = 9.1, 800 MEPPs; (*C*) t = 28.5 min, γ = 2.4, 617 MEPPs; (*D*) t = 42.5 min, γ = 3.2, 517 MEPPs; t = 50.5 min (not shown), γ = 4.0, 621 MEPPs; (*E*) t = 58.5 min, γ = 4.2, 409 MEPPs. The average values (mV) of the peak amplitudes of the control, early (<5 min), and late (>29 min) La^{3+} were, respectively: 0.34 ± 0.11, 0.64 ± 0.23 and 0.42 ± 0.09. Histogram *C* may be in error because $\langle r \rangle$ was rather high when the data were collected.

We are indebted to Professor Bruce W. Knight, Jr. for many hours of fruitful discussion, his steady encouragement, and sound advice. We thank Paul Rosen for assembling and maintaining the computer.

This work was supported by U.S. Public Health Service grant NS18354 (W.P.H.), and by grants from the Veterans Administration (J.R.S.) and the Muscular Dystrophy Association (B.C.).

Original version received 6 August 1985 and accepted version received 20 December 1985.

REFERENCES

Bendat, J. S., and A. G. Piersol. 1971. Random Data: Analysis and Measurement. John Wiley & Sons, Inc., New York. 471 pp.

Campbell, N. 1909. The study of discontinuous phenomena. *Proceedings of the Cambridge Philosophical Society.* 15:117–136.

Carlson, C. G., and M. E. Kriebel. 1985. Neostigmine increases the size of subunits composing the quantum of transmitter release at mouse neuromuscular junction. *Journal of Physiology.* 367:489–502.

Ceccarelli, B., and W. P. Hurlbut. 1975. The effects of prolonged repetitive stimulation in hemicholinium on the frog neuromuscular junction. *Journal of Physiology.* 247:163–188.

Ceccarelli, B., and W. P. Hurlbut. 1980. Ca^{2+}-dependent recycling of synaptic vesicles at the frog neuromuscular junction. *Journal of Cell Biology.* 87:297–303.

Clark, A. W., W. P. Hurlbut, and A. Mauro. 1972. Changes in the fine structure of the neuromuscular junction of the frog caused by black widow spider venom. *Journal of Cell Biology.* 52:1–14.

del Castillo, J., and D. W. Pumplin. 1975. Discrete and discontinuous action of brown widow spider venom on the presynaptic nerve terminals of frog muscle. *Journal of Physiology.* 252:491–508.

Eisenberg, R. S. 1983. Impedance measurement of the electrical structure of skeletal muscle. *In* Handbook of Physiology, Section 10: Skeletal Muscle. L. D. Peachy, editor. Williams & Wilkins Co., Baltimore, MD.

Fesce, R., J. R. Segal, B. Ceccarelli, and W. P. Hurlbut. 1985. Measurement of the rate of quantal secretion induced by black widow spider venom (BWSV) at the endplate. *Biophysical Journal.* 47(2, Pt. 2):477*a*. (Abstr.)

Fesce R., J. R. Segal, and W. P. Hurlbut. 1986. Fluctuation analysis of nonideal shot noise. Application to the neuromuscular junction. *Journal of General Physiology.* 88:25–57.

Finger, W. 1984. High rates of excitatory miniature currents in crayfish claw opener muscle evoked by high concentrations of γ-aminobutyric acid (GABA) in normal and Ca^{2+}-deficient superfusions. *Neuroscience Letters.* 47:251–256.

Finger, W., and H. Stettmeier. 1981. Analysis of miniature spontaneous inhibitory postsynaptic currents (sIPSCs) from current noise in crayfish opener muscle. *Pflügers Archiv European Journal of Physiology.* 392:157–162.

Finkelstein, A., L. L. Rubin, and M.-C. Tzeng. 1976. Black widow spider venom: effect of purified toxin on lipid bilayers. *Science.* 193:1009–1011.

Florey, E., and M. A. Cahill. 1982. The innervation pattern of crustacean skeletal muscle. Morphometry and ultrastructure of terminals and synapses. *Cell and Tissue Research.* 224:527–541.

Frontali, N., B. Ceccarelli, A. Gorio, A. Mauro, P. Siekevitz, M.-C. Tzeng, and W. P. Hurlbut. 1976. Purification from black widow spider venom of a protein factor causing the depletion of synaptic vesicles at neuromuscular junctions. *Journal of Cell Biology.* 68:462–479.

Gorio, A., W. P. Hurlbut, and B. Ceccarelli. 1978. Acetylcholine compartments in mouse diaphragm. Comparison of the effects of black widow spider venom, electrical stimulation and high concentrations of potassium. *Journal of Cell Biology.* 78:716–733.

Haimann, C., F. Torri-Tarelli, R. Fesce, and B. Ceccarelli. 1985. Measurement of quantal secretion induced by ouabain and its correlation with depletion of synaptic vesicles. *Journal of Cell Biology.* 101:1953–1965.

Katz, B. 1978. The release of the neuromuscular transmitter and the present state of the vesicular hypothesis. *In* Studies in Neurophysiology. Cambridge University Press, Cambridge. 1–21.

Katz, B., and R. Miledi. 1972. The statistical nature of the acetylcholine potential and its molecular components. *Journal of Physiology.* 224:665–699.

Kawai, N., A. Mauro, and H. Grundfest. 1972. Effect of black widow spider venom on the lobster neuromuscular junctions. *Journal of General Physiology.* 60:650–664.

Kriebel, M. E., and E. Florey. 1983. Effect of lanthanum ions on the amplitude distributions of miniature endplate potentials and on synaptic vesicles in frog neuromuscular junctions. *Neuroscience.* 9:535–547.

Kriebel, M. E., and C. E. Gross. 1974. Multimodal distribution of frog miniature enplate potentials in adult, denervated, and tadpole leg muscle. *Journal of General Physiology.* 64:85–103.

Larkin, J. M., M. S. Brown, J. L. Goldstein, and R. G. W. Anderson. 1983. Depletion of intracellular potassium arrests coated pit formation and receptor-mediated endocytosis in fibroblasts. *Cell.* 33:273–285.

Letinsky, M. S., K. H. Fishbeck, and U. J. McMahan. 1976. Precision of reinnervation of original post-synaptic sites in frog muscle after a nerve crush. *Journal of Neurocytology.* 5:691–718.

Liley, A. W. 1957. Spontaneous release of transmitter substance in multiquantal units. *Journal of Physiology.* 136:595–605.

Liscum, L., P. J. Hauptman, D. C. Hood, and E. Holtzman. 1982. Effect of barium and tetraethylammonium on membrane circulation in frog retinal photoreceptors. *Journal of Cell Biology.* 95:296–309.

Longenecker, H. B., W. P. Hurlbut, A. Mauro, and A. W. Clark. 1970. Effects of black widow spider venom on the frog neuromuscular junction. *Nature.* 225:701–705.

Martin, C., and W. Finger. 1985. Tonic depolarization of excitatory nerve terminals in crayfish muscle by high concentrations of extracellular potassium. *Neuroscience Letters.* 53:309–314.

Meldolesi, J., W. B. Huttner, R. Y. Tsien, and T. Pozzan. 1984. Free cytoplasmic Ca^{2+} and transmitter release. Studies on PC 12 cells and synaptosomes exposed to α-latrotoxin. *Proceedings of the National Academy of Sciences.* 81:620–624.

Mellor, J. W. 1955. Higher Mathematics for Students of Chemistry and Physics. Dover Publications, Inc., New York. 641 pp.

Misler, S., and W. P. Hurlbut. 1979. Action of black widow spider venom on quantized release of acetylcholine at the frog neuromuscular junction: dependence upon external Mg^{2+}. *Proceedings of the National Academy of Sciences.* 76:991–995.

Nakajima, Y., and T. S. Reese. 1983. Inhibitory and excitatory synapses in crayfish receptor organs studied with direct rapid-freezing substitution. *Journal of Comparative Neurology.* 213:66–73.

Nicholls, D. G., M. Rugolo, I. G. Scott, and J. Meldolesi. 1982. α-Latrotoxin of black widow venom depolarizes the plasma membrane, induces massive calcium influx, and stimulates transmitter release in guinea pig brain synaptosomes. *Proceedings of the National Academy of Sciences.* 79:7924–7928.

Peper, K., F. Dreyer, C. Sandri, K. Akert, and H. Moor. 1974. Structure and ultrastructure of the frog motor endplate. A freeze-etching study. *Cell and Tissue Research.* 149:437–455.

Rice, S. O. 1944. Mathematical analysis of random noise. *Bell Technical Systems Journal.* 23:282–332.

Segal, J. R., B. Ceccarelli, R. Fesce, and W. P. Hurlbut. 1985. Miniature endplate potential frequency and amplitude determined by an extension of Campbell's theorem. *Biophysical Journal.* 47:183–202.

Shick, K. L. 1974. Power spectra of pulse sequences and implications for membrane fluctuations. *Acta Biotheoretica.* 23:1–17.

Smith, J. E., A. W. Clark, and R. A. Kuster. 1977. Suppression by elevated calcium of black widow spider venom activity at frog neuromuscular junction. *Journal of Neurocytology*. 6:519–539.

Valtorta, F., L. Madeddu, J. Meldolesi, and B. Ceccarelli. 1984. The receptor for α-latrotoxin is an externally exposed protein of the presynaptic membrane. *Journal of Cell Biology*. 99:124–132.

Verveen, A. A., and L. J. de Felice. 1974. Membrane noise. *Progress in Biophysics and Molecular Biology*. 28:189–268.